XII. PHYSICAL ACOUSTICS*

Prof. K. U. Ingard
Prof. L. W. Dean III
Dr. G. C. Maling, Jr.
Dr. H. L. Willke, Jr.
P. A. Fleury V
K. W. Gentle
J. L. Macon
A. A. Maduemezia
W. M. Manheimer
M. A. Martinelli
J. A. Ross
T. B. Smith
S. D. Weiner

RESEARCH OBJECTIVES

Our general objective involves the study of the emission, propagation, and absorption of sound and vibrations in matter. Specific areas of current research in fluids include generation and propagation of sound waves in ionized gases, nonlinear acoustics and shock waves, and problems dealing with acoustic and flow instabilities.

K. U. Ingard

A. HYPERSONIC VELOCITY AND ABSORPTION IN LIQUIDS

The Brillouin scattering of the highly monochromatic and well-collimated light from an He-Ne laser has been used to obtain measurement of sound velocity and absorption in the kMc range.[1] Extensions of this type of measurement are reported here, in which the phonon frequencies investigated varied from 1 to 5 kMc. Preliminary results indicate the possible existence of a resonant molecular absorption of sound waves.

Brillouin scattering results from the interaction of light with thermal fluctuations in the density, and hence the refractive index, of the medium. If such density fluctuations are represented as a gas of phonons, the scattering is then fruitfully viewed as a photon-phonon collision in which a phonon is either created (anti-Stokes) or destroyed (Stokes). Conservation of energy and momentum, along with the observation that $v_s \ll c$ result in the relations:

$$\pm\omega_s = \Delta\omega = \omega_o - \omega'$$

$$k_s = \Delta k = \pm\left|\vec{k}_o - \vec{k}'\right| = \pm 2k_o \sin\frac{\theta}{2}$$

$$\omega_s = \Delta\omega = \pm 2\omega_o \frac{\eta v_s}{c} \sin\frac{\theta}{2},$$

where ω_o, ω', ω_s are frequencies of incident and scattered light and sound, respectively, θ is the scattering angle, v_s is the sound velocity, and η is the medium's refractive index.

For a perfectly monochromatic light beam, any observed spread in ω_s could be attributed to the finite phonon lifetimes (that is, sound absorption). The actually observed width of the Brillouin line $\delta\nu$ is composed of the sound-absorbing contribution and the

*This work was supported in part by the U. S. Navy (Office of Naval Research under Contract Nonr-1841(42)).

frequency spread of the maser. These widths are additive if Lorentzian line shapes are assumed.

$$\delta\nu = \delta\nu_n + \delta\nu_s.$$

The relation $\left(\frac{\delta\nu_s}{\Delta\nu}\right)\frac{2\pi}{\lambda_s} = \alpha_s$ determines the sound absorption coefficient α_s, where λ_s is the sound wavelength, and $\Delta\nu$ is the interorder spacing of the Fabry-Perot interferometer.

The experiment is schematically represented in Fig. XII-1. Slow pressure scanning of the Fabry-Perot results in a recorder output such as appears in Fig. XII-2. For these experiments the maser width was ~720 Mc, the maser power, 10-20 mW. The temperature was 22-23°C resulting in a spread of velocities of ±1.0 per cent because of lack of temperature control. The variation of the angle θ and hence of the frequency ω_s was achieved by reflecting the incident light from an adjustable mirror

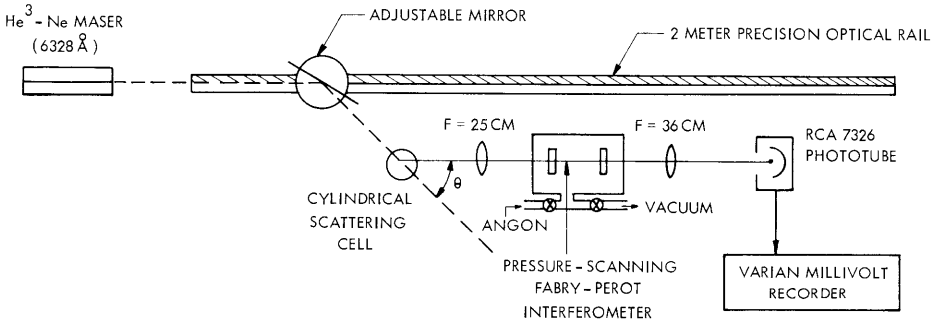

Fig. XII-1. Experimental apparatus. The maser is linearly polarized perpendicularly to the scattering plane.

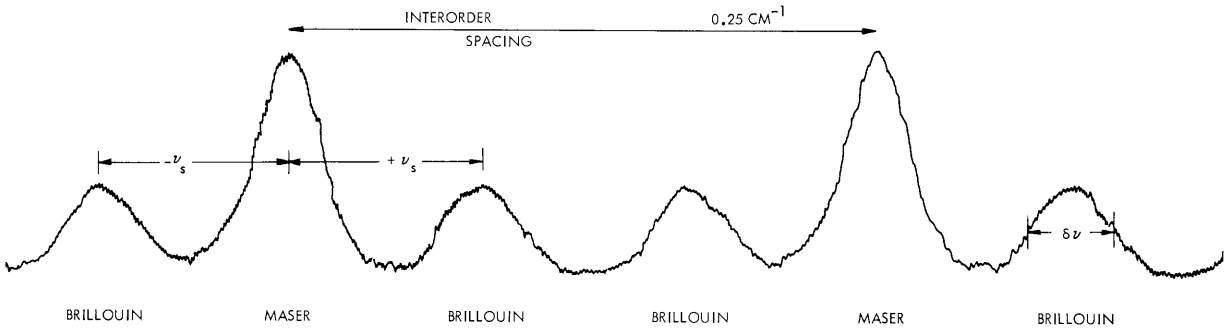

Fig. XII-2. Recorder trace of spectrum in acetic acid at θ = 60°; T = 23°C.

mounted on a moveable spectroscopic table. The angles could be measured to better than 0.1°.

Because of the magnitude of the maser linewidth and variations in the maser power, the accuracy of absorption measurements is no better than ~10 percent. At such frequencies (~5 kMc), however, absorption is so high that conventional ultrasonic (propagation) techniques could not be expected to serve very well. The accuracies in this experiment could be improved by narrowing the maser width, using lock-in detection, and increasing the finesse of the Fabry-Perot interferometer.

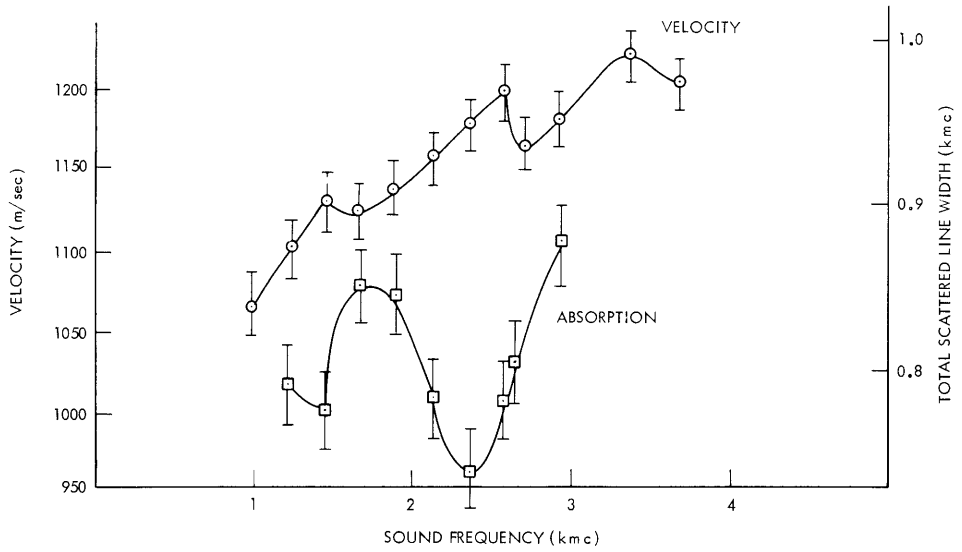

Fig. XII-3. Hypersonic velocity and absorption in acetic acid.

Measured values of absorption coefficients and speed of sound for acetic acid are presented in Fig. XII-3. Salient features are the nonmonatomic behavior of velocity, the peak in the absorption at ~175 kMc, and the correspondence between absorption and velocity data, which would be expected from Kramers-Kronig relations; however, on account of the magnitude of the error, caution should be exercised in interpreting these results.

Departure observed from classical absorption and velocity dispersion in liquids has heretofore been of the relaxational type.[2] Our results indicate the possibility of a resonant molecular sound-absorption mechanism. Refinements of apparatus and technique are under way, and reduction of experimental errors will make possible more definite conclusions regarding resonances. Meanwhile, Brillouin scattering stands out as the best, and sometimes the only, technique for studying the propagation characteristics of kilomegacycle sound.

This experiment was performed jointly with R. Y. Chiao, of the Optical Maser Group,* M. I. T., which is under the direction of Professor C. H. Townes and Professor A. Javan.

P. A. Fleury V

References

1. R. Y. Chiao and B. P. Stoicheff, J. Opt. Soc. Am. 54, 1286 (1964); G. B. Benedek, J. B. Lastovka, K. Fritsch, and T. Greytak, J. Opt. Soc. Am. 54, 1284 (1964).

2. K. F. Herzfeld and T. A. Litovitz, Absorption and Dispersion of Ultrasonic Waves (Academic Press, New York, 1959).

B. LONGITUDINAL WAVES IN A WEAKLY IONIZED GAS

We have reported elsewhere[1] on an experiment in which the neutral gas temperature in the plasma column of an argon discharge was determined from sound-velocity measurements with Langmuir probes used as acoustic detectors. The analysis of the data obtained was based on the assumption that the measured wave velocity was the same as that in un-ionized argon. In the present report the validity of this assumption is investigated by an analysis of the different longitudinal modes that can exist in the weakly ionized gas.

This analysis is based on the following set of linearized equations of motion in which the subscripts n, i, and e refer to the neutrals, the ions, and the electrons, respectively.

$$
\begin{aligned}
&\partial_t n_n + N_n \partial_x v_n = 0 \\
&\partial_t v_n + \rho_n^{-1} \partial_x p_n = \omega_{ni}(v_i - v_n) + \omega_{ne}(v_e - v_n) \\
&\partial_t n_i + N_i \partial_x v_i = 0 \\
&\partial_t v_i + \rho_i^{-1} \partial_x p_i = \omega_{in}(v_n - v_i) + (q/m_i)e + \omega_{ie}(v_e - v_i) \\
&\partial_t n_e + N_e \partial_x v_e = 0 \\
&\partial_t v_e + \rho_e^{-1} \partial_x p_e = \omega_{en}(v_n - v_e) - (q/m_e)e + \omega_{ei}(v_i - v_e) \\
&\partial_x e = 4\pi q(n_i - n_e), \qquad N_i = N_e \\
&p_n = c_n^2 m_n n_n \qquad p_i = c_i^2 m_i n_i \qquad p_e = c_e^2 m_e n_e.
\end{aligned}
\tag{1}
$$

*The research of this group is supported in part by the National Aeronautics and Space Administration.

Here, N stands for particle density; p, v, n, and e are perturbations in pressure, flow velocity, density, and electric field, respectively; q is the electronic charge; m is the particle mass; and $\rho = Nm$ is the density. The coupling between the three fluid components is expressed by the collision terms on the right-hand side of the momentum equations. The collision frequencies involved are related as follows:

$$\omega_{ne} = (N_e m_e / N_n m_n)\omega_{en}, \qquad \omega_{ni} = (N_i m_i / N_n m_n)\omega_{in} \approx (N_i / N_n)\omega_{in}$$
$$\omega_{in} = /m_e/m_i)\omega_{ei}. \tag{2}$$

Under the conditions of interest here, with gas pressures of the order of 1 Torr and electron densities of the order of 10^{10} cm^{-3}, we find that the frequencies ω_{ni} and ω_{ne} are approximately unity or less, ω_{en}, ω_{in}, and ω_{ei} are of the order of 10^5 or larger, and ω_{ie} is of the order of 10^2 sec^{-1}. The plasma frequencies for the electrons and the ions, ω_e and ω_i, are of the order of 10^{10} and 10^8 sec^{-1}, respectively. Thus, within the frequency range of interest here, between 10^2 and 10^5, we have $(\omega_{ne}, \omega_{ni}) \ll \omega \ll (\omega_e, \omega_i)$.

Since the basic object of this analysis is to investigate the influence of the collisions between the neutrals and the charged particles on the acoustic-wave mode, we have not included viscous stress terms in the momentum equation, or the influence of heat conduction. Accordingly, the pressures p_n, p_i, and p_e have been set proportional to the respective densities, with the constant of proportionality c^2 essentially being the inverse of the compressibility of the various components, $c^2 = 1/\rho\kappa$.

The dispersion relation for plane waves resulting from the equations of motion indicates the existence of three longitudinal wave modes.

The first mode with the dispersion relation

$$k = \omega / c_n \tag{3}$$

is the ordinary sound wave that travels with the sound speed of the neutral gas, c_n. There is no damping resulting from n-i and n-e collisions which is of any consequence in comparison with the ordinary damping caused by viscosity and heat conduction. (It should be pointed out that to obtain the correct damping terms and eigenvectors, it is essential to keep all terms of the order of ω_{ni}/ω and ω_{ne}/ω and defer approximations until calculations are completed. Otherwise there may be misleading results.[2] In this acoustic mode all three fluid components have the same amplitude and move in phase with each other, and the relative change in density for all components is the same. Since they all move together, there is no momentum transfer from one component to the other.

The second mode with the dispersion relation

$$k^2 \approx k_o^2 \left[1 + i \frac{\omega_{in}}{\omega}\right] \tag{4}$$

can be regarded as a degenerate ion acoustic wave. In this mode the ions and the

electrons move in phase with each other with the same amplitude, and the neutrals can be considered to be at rest. Actually, the velocity amplitude of the neutrals is of the order of N_i/N_o, that is, negligible compared with the amplitude of the charge components. The wave amplitude decays within one acoustic wavelength.

The third mode is a degenerate plasma oscillation with a dispersion relation

$$k^2 = (\omega/c_n)^2 \left[-(\omega_e/\omega)^2 + i \frac{\omega_{en} + \omega_{in}}{\omega} + i(T_e \omega_{in}/\omega T_i) \right] (T_i/T_e), \tag{7}$$

or

$$k \approx i \frac{\omega_e}{c_n} \sqrt{\frac{T_i}{T_e}}.$$

In this mode the neutrals are approximately stationary, and the ions and electrons move in opposite directions with the same amplitudes. The wavelength is of the order of the Debye length, and the motion is overdamped.

Our analysis has shown that of the three possible longitudinal modes only the acoustic mode will propagate without significant attenuation through the ionized gas, and that the presence of charged particles does not influence the speed and attenuation of this mode. The collisions are sufficiently frequent to "freeze" the ions and electrons to the neutrals in this wave mode. The two remaining modes are strongly damped and should attenuate within approximately one wavelength of the sound wave and a Debye length, respectively.

K. W. Gentle, K. U. Ingard

References

1. K. W. Gentle and U. Ingard, Appl. Phys. Letters 5, 105 (1964).

2. G. M. Sessler, Phys. Fluids 7, 90 (1964) contains references to other relevant papers.

C. COUPLING OF DIFFUSION AND PRESSURE WAVES IN A WEAKLY IONIZED GAS

An attempt will be made to explain stationary striations in the positive column of a gas discharge in terms of coupling of diffusion and pressure waves. In this analysis, the electrons are assumed to diffuse infinitely rapidly relative to the ions and form a uniform negative background. The equations of motion for the ions are then linearized in the quantities n, v, and e, representing the perturbations in ion density, ion velocity, and longitudinal electric field. Transverse variations are neglected and one-dimensional equations are used:

$$n_t + Vn_x + Nv_x = \gamma Ne$$

$$e_x = qn \tag{2}$$

$$Nv_t + NVv_x + c^2 n_x - \frac{Nq}{m} E - \frac{qe}{m} n = 0 \tag{3}$$

where V is the ion drift speed, N is the unperturbed ion density, q is the electronic charge, E is the unperturbed electric field, c is the ion sound speed, and γ is $\partial Z/\partial E$, where Z is the ionization rate. Combining Eqs. 1-3 gives an equation for n:

$$n_{ttx} + 2Vn_{txx} - (c^2 - V^2)n_{xxx} - \gamma qN(n_t + Vn_x) + \frac{Nq^2}{m} n_x + i\frac{V}{\tau_i} n_{xx} = 0, \tag{4}$$

and a dispersion relation

$$\omega^2 - 2V\omega k - (c^2 - V^2)k^2 - \frac{\gamma qN}{k}(\omega - Vk) - \frac{Nq^2}{m} - i\frac{V}{\tau_i} k = 0, \tag{5}$$

where τ_i is the ion-neutral collision time. The term, Nq^2/m, is the square of the ion plasma frequency, while the imaginary term, iVk/τ_i, produces damping of the waves. From Eq. 5, the group velocity is found to be

$$V_{gr} = V - (V_D/2) \pm \frac{c^2 - (V_D/2)^2 + i(V/2\tau_i k)}{\sqrt{c^2 + (V_D/2)^2 + (Nq^2/mk^2) + i(V/\tau_i k)}}, \tag{6}$$

where $V_D = \gamma qN/k^2$. It is expected that stationary striations will be observed with values of k corresponding to $V_{gr} = 0$. It might be mentioned that $V_{ph} = 0$ for k of the same order of magnitude. Before attempting to solve Eq. 6 to find k when $V_{gr} = 0$, it is advantageous to consider the orders of magnitude of the various velocities entering into Eq. 6. We shall find an approximate solution of Eq. 6 for an Argon plasma. In this case, the terms c^2, V_D^2, and $V/\tau_i k$ are kept, while the terms V^2, and Nq^2/mk^2 are dropped. Thus

$$V_{gr} = -V_D/2 \pm \frac{c^2 - (V_D/2)^2 + i(V/2\tau_i k)}{\sqrt{c^2 + (V_D/2)^2 + i(V/\tau_i k)}}. \tag{7}$$

Since we are interested in observing stationary striations, we require that Re $(V_{gr}) = 0$, but we do not impose any conditions on Im (V_{gr}).

It is convenient to consider the solution to Eq. 7 in the two limiting regions, $c^2 \gg V/\tau_i k$ and $c^2 \ll V/\tau_i k$.

Case 1: $c^2 \gg V/\tau_i k$

Making this approximation in Eq. 7 gives

$$\mathrm{Re}\,(V_{gr}) = -V_D/2 \pm \frac{c^2 - (V_D/2)^2}{\sqrt{c^2 + (V_D/2)^2}} + \text{terms of order } \left[\frac{V/\tau_i k}{c^2}\right]^2 c. \tag{8}$$

This has Re $(V_{gr}) = 0$ when

$$V_D = \sqrt{4/3}\, c\,.$$

This yields values of k of the same order of magnitude as experimental values (k~10).

Case 2: $c^2 \ll V/\tau_{ik}$

This case is of special interest, as it corresponds fairly well to the experimental situation and shows also the behavior of the solution as the ion temperature goes to zero. Setting c = 0 in Eq. 7 gives

$$V_{gr} = -V_D/2 \pm \frac{-(V_D/2)^2 + i(V/2\tau_i k)}{\sqrt{(V_D/2)^2 + i(V/\tau_i k)}}\,. \tag{9}$$

Equation 9 is solved by setting $(V_D/2)^2 = A(V/\tau_i k)$ to give

$$V_{gr} = \frac{\sqrt{V/\tau_i k}}{\sqrt{A^2 + 1}} \left[-\sqrt{A} \quad \sqrt{A^2 + 1} \pm (-A + i/2)\sqrt{A - i}\right]. \tag{10}$$

Substitution of numerical values for A in Eq. 10 shows that the solution Re $(V_{gr}) = 0$ occurs for A between 0 and 0.1. We use this information to make the approximation $A \ll 1$ and find that Re $(V_{gr}) = 0$ for

$$-\sqrt{A} \pm (-A/\sqrt{2} + 1/2\sqrt{2}) = 0, \tag{11}$$

with the (positive) solution

$$A = 3/2 - \sqrt{2} = 0.086. \tag{12}$$

Substituting (12) in $(V_D/2)^2 = (\gamma qN/2k^2)^2 = A(V/\tau_i k)$ gives for k

$$k^3 = \frac{(\gamma qN)^2 \tau_i}{.344V} = \frac{(\gamma qN)^2 m}{.344qE}\,. \tag{13}$$

In estimating orders of magnitude, we approximate $\gamma = dZ/dE$ by Z/E. We thus obtain

$$(kh)^3 \sim \frac{94\ mV^2}{qEh} (kT_e/qEa)^4 \sim mV^2/qEh, \tag{14}$$

where h is the Debye length, kT_e/q is the electron temperature in volts, and a is the

column radius. Putting in typical values for the parameters in Eq. 14 gives $k \sim 10\ cm^{-1}$, which is in agreement with experiment.

It should be pointed out that, although the values of k obtained in cases 1 and 2 are of the same order of magnitude, the waves in these cases differ considerably. In case 1, Im $(V_{gr}) = 0$ and the waves are undamped; in case 2, Im $(V_{gr}) \neq 0$ and the waves are damped.

It should also be mentioned that the condition Re $(V_{gr}) = 0$ does not insure that stationary striations are observed. In the case of plasma oscillations, $V_{gr} = 0$ for all k, but striations are not observed. The fact that Re $(V_{gr}) = 0$ for only one particular k, indicates, however, that if striations are observed, they should have this wave number.

S. D. Weiner, U. Ingard

D. INSTABILITY IN TIME-SYMMETRIC FLOWS

If a physical system is to appear stable against external influences, the effects of initial disturbances should not become arbitrarily magnified; in fact, eventually they must become unobservably small. It should be clear that given a system and its image under time reversal, one at most can appear stable, since the decay of an arbitrarily large initial disturbance of one system to an unobservably small level appears in the reversed system as the growth of initially unobservably small disturbances to an arbitrarily large level. In particular, a system symmetric under time reversal must be unstable. These considerations evidently apply to any systems connected by time-reversing transformations that preserve disturbance "strength" (energy, maximum amplitude or other norm) at corresponding times.

Systems unstable by symmetry are to be found among common subjects of stability theory, notably the inviscid parallel fluid flows. We shall exhibit here symmetric fluid and plasma flows together with their implemental transformations.

Solutions of the dissipation-free Navier-Stokes equations with arbitrary spatially and temporally homogeneous equations of state are apparently closed under the following transformations, with arbitrary origins for t and $\underline{x}$.

Time reversal $\quad t \rightarrow -t$

$\qquad\qquad\qquad\quad \underline{v} \rightarrow -\underline{v}$

Spatial reflection P_i: $\quad x_i \rightarrow -x_i$

$\qquad\qquad\qquad\quad v_i \rightarrow -v_i$

(Note that T and the P_i clearly preserve relevant "strength" criteria, including the L_p norms.)

Our instability criterion applies to flows that, together with their associated boundary

conditions, are invariant under a composition of T and the P_i. The most obvious application of T alone is to static equilibria, whereas P_3T, P_2P_3T, and $P_1P_2P_3T$ apply to dynamic situations with symmetric boundaries and streamlines. (Flow in more than two dimensions is not necessarily determined by its streamline pattern, so that we should specify also the symmetry of the scalar dynamical variables.) In particular,

(i) P_3T: $t \to -t$

$x_3 \to -x_3$

$v_j \to -v_j \qquad j \neq 3$

leaves invariant stationary or otherwise time-symmetric flows with streamlines symmetric in x_3, including any parallel flow of the form $\underline{V} = \underline{\epsilon}_3 W(x_1, x_2)$, in which W may be discontinuous (tangential shocks), or such flow altered by the introduction of objects symmetric in x_3. P_3T also transforms normal shocks with higher pressure behind the shock into normal shocks with higher pressure ahead of the shock, which shows that at least one type is unstable.

(ii) P_2P_3T: $t \to -t$

$x_2 \to -x_2$

$x_3 \to -x_3$

$v_1 \to -v_1$

applies to time-symmetric flows in three spatial dimensions invariant under 180° rotation about the x_1 axis, including that over rotation-symmetric wings and airfoils, or such flow modified by steadily rotating fans and propellers with such symmetry at t = 0.

(iii) $PT = \pi_i P_i T$ $\qquad t \to -t$

$\underline{x} \to -\underline{x}$

leaves invariant symmetric flow over a yawed tipped flat rectangular plate or other object symmetric through the origin.

The addition of $B_i \to -B_i$ to the P_i extends these transformations to encompass perfectly conducting plasmas. Another invariance property,

Charge conjugation C: $\underline{B} \to -\underline{B}$

$\underline{j} \to -\underline{j}$

also appears. All equilibrium plasma configurations, regardless of field and current profiles and boundary conditions, are symmetric under T itself, and hence

unstable. Dynamic plasma situations are to be handled after the fashion of the fluid flows discussed above.

H. L. Willke, Jr.

E. SHOCK-WAVE TRANSMISSION AND ATTENUATION

A longer driver for the shock tube described in a previous report[1] has been constructed. Also, a new microphone system has been installed which has a frequency

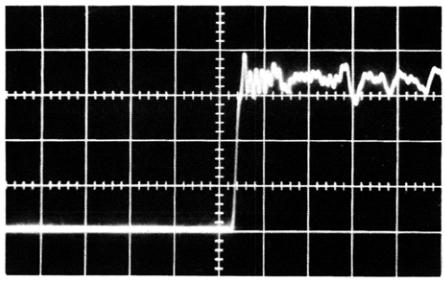

Fig. XII-4. Pressure signature of a shock wave incident on the end of the tube. Horizontal sweep speed ≐0.2 msec/cm.

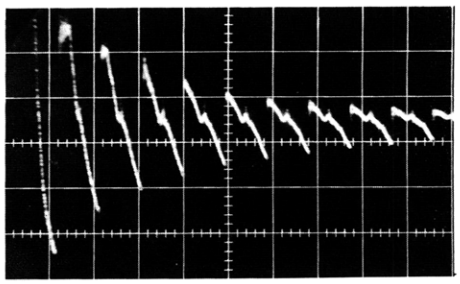

Fig. XII-5. Decay of a shock wave in the tube. Horizontal sweep speed ≐2 msec/cm.

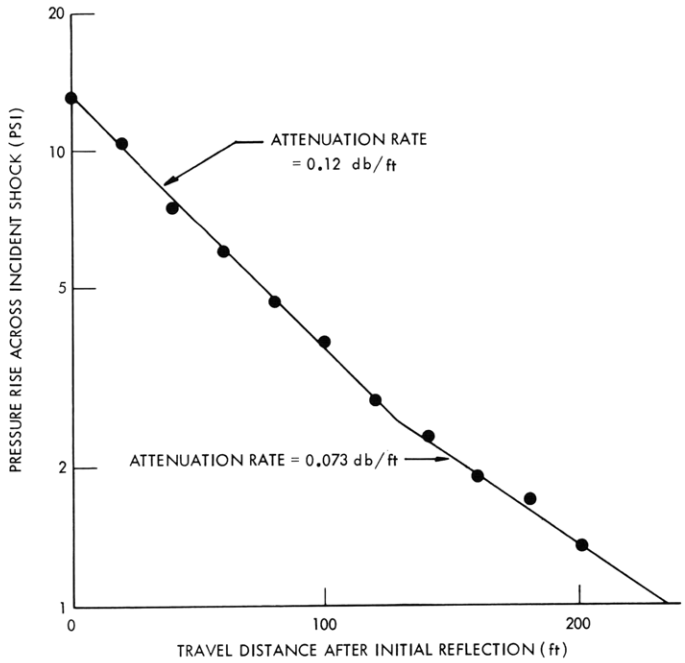

Fig. XII-6. Shock decay rate as a function of travel distance.

response from 0 to 10 kc, and allows us to measure pressures up to 100 psi. A static-pressure gauge can therefore be used for calibration.

Experiments with the new system have confirmed the data presented previously[1] on the pressure reduction produced by a fine screen in the tube. A typical photograph of the pressure signature measured at the end of the tube (closed) is shown in Fig. XII-4. The wall pressure produced by this shock wave is 32 psi. Some measurements have also been made of the decay of a shock wave as it is reflected from the closed ends of the tube. Some typical results are shown in Fig. XII-5. Here, the incident pulse is too large to be seen on the screen, but its amplitude was obtained from other photographs. The decay of the wave must be calculated from a measurement of pressure at the end of the tube because the nonlinear interaction of the incident and reflected waves must be taken into account. Some preliminary decay data have been calculated from this photograph, and are shown in Fig. XII-6. The decay rate is faster than that calculated for repeated shock waves in free space.[2]

G. C. Maling, Jr., U. Ingard

References

1. G. C. Maling, Jr. and U. Ingard, Quarterly Progress Report No. 75, Research Laboratory of Electronics, M. I. T., October 15, 1964, pp. 42-44.

2. I. Rudnick, J. Acoust. Soc. Am. 25, 1012 (1953).